

NASA TECHNICAL NOTE



NASA TN D-5115

c. 1

NASA TN D-5115



LOAN COPY: RETURN TO
AFWL (WLIL-2)
KIRTLAND AFB, N MEX

EFFECT OF FLOW RATE ON THE DYNAMIC CONTACT ANGLE FOR WETTING LIQUIDS

by Thom A. Coney and William J. Masica

Lewis Research Center

Cleveland, Ohio



EFFECT OF FLOW RATE ON THE DYNAMIC CONTACT
ANGLE FOR WETTING LIQUIDS

By Thom A. Coney and William J. Masica

Lewis Research Center
Cleveland, Ohio

NATIONAL AERONAUTICS AND SPACE ADMINISTRATION

For sale by the Clearinghouse for Federal Scientific and Technical Information
Springfield, Virginia 22151 - CFSTI price \$3.00

ABSTRACT

Experimental measurements were made of the dynamic contact angle over a previously wetted liquid surface as a function of interface velocity and liquid properties. The experiments were conducted in a weightless environment using glass tubing with a rectangular cross section. All liquids exhibited zero degree static contact angles. The study showed that existing theory adequately predicted the contact angle dependence on interface velocity and liquid properties. In addition, qualitative agreement was obtained between the theoretical and experimental interface shapes.

EFFECT OF FLOW RATE ON THE DYNAMIC CONTACT ANGLE FOR WETTING LIQUIDS

by Thom A. Coney and William J. Masica
Lewis Research Center

SUMMARY

Experimental measurements were made of the dynamic contact angle over a previously wetted liquid surface as a function of interface velocity and liquid properties. The experiments were conducted in a weightless environment using rectangular glass tubing (1.0×0.25 cm in cross section). Interface velocities ranged from 1.4 to 28 centimeters per second. Liquid properties included surface tensions from 16.6 to 24.4 dynes per centimeter and viscosities from 0.56 to 6.7 centipoise. Liquids exhibited zero degree static contact angles. The study showed that existing theory adequately predicted the contact angle dependence on interface velocity and liquid properties. In addition, qualitative agreement was obtained between the theoretical and experimental interface shapes.

INTRODUCTION

The angle of contact of a liquid-vapor interface at a surface depends on the motion of the liquid relative to the surface. The particular angle considered here is referred to as the dynamic contact angle and is defined as the angle formed by the advancing liquid-vapor interface as the interface moves at a constant velocity relative to a surface. (Dynamic contact angle should not be confused with contact angle hysteresis which refers to the difference between advancing and receding angles.) The surface may be either a dry solid or a wetting layer of liquid. In either case it is generally accepted that the dynamic contact angle not only differs from the static angle but also that it varies as a function of the interface velocity. This velocity dependence was demonstrated experimentally for flow over a dry surface by Rose and Heinz (ref. 1) and theoretically for flow over a previously wetted surface by G. Friz (ref. 2). Friz compared his predicted relation to the experimental data obtained by Rose and Heinz. But because these data

were obtained for flow over a dry surface, a basic condition of the theory, that the surface be previously wetted, was not satisfied.

The purpose of this experiment was to obtain data that better satisfy the conditions of Friz's analysis and to test the theory proposed. The experiment was conducted in a weightless environment (effective gravitational acceleration $<10^{-5} g$) using glass tubing with a rectangular cross section. Conducting the experiment in this manner simplified the contact angle measurement and enhanced the formation of the standing wave form in the wall layer of liquid preceding the advancing meniscus. All liquids used exhibited zero degree static contact angles.

The result of this experiment may have specific application in the area of low-gravity liquid-propellant sloshing. It is known that the sloshing frequencies and damping are dependent on the contact angle as well as the liquid properties, depth, and container shape (refs. 3 and 4). Therefore, an acceptable theory predicting the functional dependence of the contact angle on the liquid edge velocity at the container wall will provide information needed in the further development of slosh theory.

SYMBOLS

A	dimensionless constant, $A = 3u_0 \eta / \sigma$
$a(x), b(x)$	coefficients in expansion of u
d	characteristic length in Reynolds number, cm
g	acceleration due to gravity, $g = 981 \text{ cm/sec}^2$
k	dimensionless coordinate, l/l_∞
k'''	third derivative of k , d^3k/dq^3
l	layer thickness, cm
p	pressure, N/m^2
Δp	pressure difference between vapor and liquid phases, N/m^2
q	dimensionless coordinate, x/l_∞
R	surface radius, cm
Re	Reynolds number, $\text{Re} = \frac{\rho du_0}{\eta}$
t	time, sec
u	x-component of the interface velocity, cm/sec
\vec{v}	vector interface velocity, cm/sec

x, y	rectangular Cartesian coordinates, cm
α	problem constant
η	viscosity, cP
θ	dynamic contact angle, deg
ρ	density, g/cm ³
σ	surface tension, dyne/cm
τ	shear stress, N/m ²

Subscripts:

0, 1, 2, 3	integers denoting constants
∞	infinite condition

THEORY

The Theoretical Analysis Performed by Friz (Ref. 2)

The problem that was analyzed by G. Friz and that is summarized here is illustrated in figure 1. In the figure a liquid slug is shown moving through a pipe at a constant interface velocity u_0 . The inside surface of the pipe was assumed ideally smooth and previously wetted with a layer of liquid of constant thickness l_∞ . The coordinate axes were chosen with the x axis along the pipe wall and moving with the liquid slug at velocity u_0 .

The region of interest, enclosed in the dashed rectangle, included the dynamic contact angle θ and the standing wave formed in the liquid layer preceding the advancing interface. The curvature at the center portion of the interface was not considered. The analysis was limited to steady, two-dimensional flow with negligible body forces. This and appropriate linearization reduced the Navier-Stokes equation

$$\rho \left[(\vec{v} \cdot \nabla) \vec{v} + \frac{d\vec{v}}{dt} \right] = \rho \vec{g} - \nabla p + \eta \nabla^2 \vec{v} \quad (1)$$

to the form

$$\frac{1}{\eta} \frac{\partial p}{\partial x} = \frac{\partial^2 u}{\partial y^2} \quad (2)$$

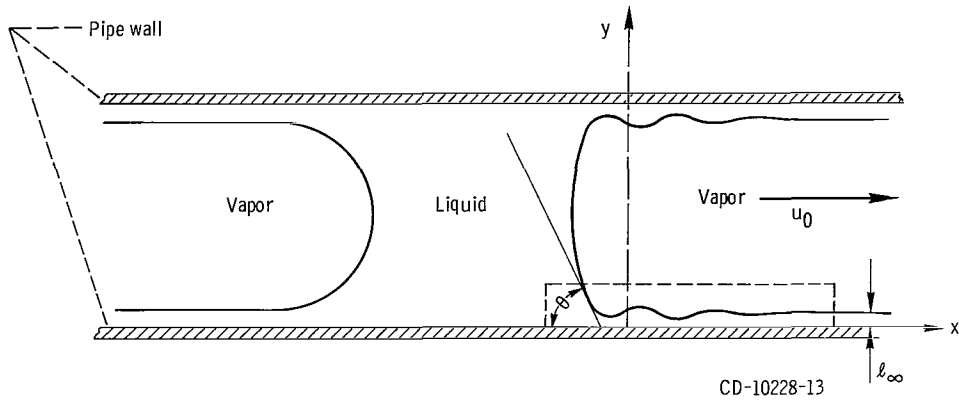


Figure 1. - Interface shape of a liquid slug advancing through a pipe.

where η is the liquid viscosity and u is the flow velocity in the x direction. The above conditions imply creeping viscous flow; thus, equation (2) is rigorously applicable only for Reynolds numbers $\ll 1$. Equation (2) is valid for the wall streamline at u equals a constant and y equals zero.

Consider first the right-hand side of equation (2). The profile for the x -component of the velocity is given by an equation of the form

$$u = -u_0 + a(x)y + b(x)y^2 \quad (3)$$

with

$$\frac{\partial^2 u}{\partial y^2} = 2b(x)$$

The liquid layer thickness is given by $l = l(x)$. Assuming that for large x the interface curvature damps to zero and friction shear stresses vanish, the continuity condition requires

$$\int_0^l u dy = -u_0 l + \frac{a(x)}{2} l^2 + \frac{b(x)}{3} l^3$$

and that

$$\int_0^l u dy = -u_0 l_\infty$$

where l_∞ is the asymptotically reached constant layer thickness. Therefore,

$$-u_0 l_\infty = -u_0 l + \frac{a(x)}{2} l^2 + \frac{b(x)}{3} l^3 \quad (4)$$

For all values of x , the shear stress on the interface must be zero,

$$\tau_{y=l} \equiv r \left. \frac{\partial u}{\partial y} \right|_{y=l} = 0$$

Therefore, from equation (3)

$$\left. \frac{\partial u}{\partial y} \right|_{y=l} = a(x) + 2b(x)l = 0 \quad (5)$$

Using equations (4) and (5), an expression for $b(x)$ can be obtained:

$$b(x) = \left(\frac{3u_0}{2l_\infty^2} \right) \left[\frac{1 - \frac{l}{l_\infty}}{\left(\frac{l}{l_\infty} \right)^3} \right] \quad (6)$$

Substituting this into equation (3) yields

$$\frac{\partial^2 u}{\partial y^2} = \frac{3u_0}{l_\infty^2} \left[\frac{1 - \frac{l}{l_\infty}}{\left(\frac{l}{l_\infty} \right)^3} \right]$$

Equation (2) then becomes

$$\frac{1}{\eta} \frac{\partial p}{\partial x} \Big|_{y=0} = \frac{3u_0}{l_\infty^2} \left[\frac{1 - \frac{l}{l_\infty}}{\left(\frac{l}{l_\infty}\right)^3} \right] \quad (7)$$

Thus, the right side of equation (2) is now a function only of $l(x)$. The same remains to be done for the left side. Assuming a constant liquid-vapor surface tension, the pressure can be related to $l(x)$ by the Laplace capillarity equation

$$\Delta p = \frac{\sigma}{R} \quad (8)$$

where Δp is the pressure difference between the vapor and liquid phases and R is the principal radius of curvature at a given point of the two-dimensional interface. The total curvature can be written exactly as

$$\frac{1}{R} = \frac{\frac{d^2 l}{dx^2}}{\left[1 + \left(\frac{dl}{dx}\right)^2 \right]^{3/2}} \quad (9)$$

Friz's analysis assumed that dl/dx is sufficiently small so that $(dl/dx)^2 \approx 0$. Equation (8) becomes

$$\Delta p = \sigma \frac{d^2 l}{dx^2}$$

and

$$\frac{d(\Delta p)}{dx} = - \frac{dp}{dx} = \sigma \frac{d^3 l}{dx^3} \quad (10)$$

assuming that the vapor pressure is constant. For creeping viscous flow, $(\partial p / \partial y)_x = 0$. Therefore, $p|_{y=l} = p|_{y=0}$ which also implies that $(dp/dx)_{y=l} = (\partial p / \partial x)_{y=0}$ or from equation (10)

$$\left. \frac{\partial p}{\partial x} \right|_{y=0} = -\sigma \frac{d^3 l}{dx^3} \quad (11)$$

The final combination of equations (2), (7), and (11) yields

$$\frac{d^3 l}{dx^3} + \left(\frac{3u_0 \eta}{\sigma} \right) \left[\frac{1 - \frac{l}{l_\infty}}{l_\infty^2 \left(\frac{l}{l_\infty} \right)^3} \right] = 0 \quad (12)$$

This equation in dimensionless form is

$$k^3 k'''' + A(1 - k) = 0 \quad (13)$$

where

$$k = \frac{l}{l_\infty}$$

$$k'''' = \frac{d^3 k}{dq^3}$$

$$q = \frac{x}{l_\infty}$$

$$A = \frac{3u_0 \eta}{\sigma}$$

The Numerical Solution to the System Differential Equation

The solution, $k = k(q)$, to equation (13) describes in dimensionless form the interface shape in the region of interest as a function of fluid properties and interface velocity. Since this solution does not exist in closed form, it was necessary to obtain the desired solution by numerical means. The particular technique used by Friz was not described.

However, his results were reproduced by the authors using the Runge-Kutta method. The analysis made use of the initial solution and the limiting conditions presented by Friz.

The initial solution for the numerical analysis was obtained by linearizing equation (13). For $k^3 \approx 1$, equation (13) became

$$k''' + A(1 - k) = 0 \quad (14)$$

having the general solution

$$k = 1 + a_1 \exp(\alpha_1 q) + a_2 \exp(\alpha_2 q) + a_3 \exp(\alpha_3 q) \quad (15)$$

where

$$\alpha_1 = |A|^{1/3}$$

$$\alpha_2 = -|A|^{1/3} \left(\sin \frac{\pi}{6} + i \cos \frac{\pi}{6} \right)$$

$$\alpha_3 = -|A|^{1/3} \left(\sin \frac{\pi}{6} - i \cos \frac{\pi}{6} \right)$$

The boundary conditions limiting k to real and finite values reduced equation (15) to a damped sinusoidal wave of the form

$$k = 1 + a_2 \exp\left(-\frac{1}{2} A^{1/3} q\right) \cos\left(\frac{\sqrt{3}}{2} A^{1/3} q\right) \quad (16)$$

Using equation (16) as the initial solution to equation (13), the numerical analysis yielded a family of curves for each value of A (see fig. 2). The two boundary conditions that the desired solution must satisfy are: (1) The standing wave preceding the advancing interface must damp to zero amplitude, i. e.,

$$\lim_{q \rightarrow \infty} k = 1 \quad (17)$$

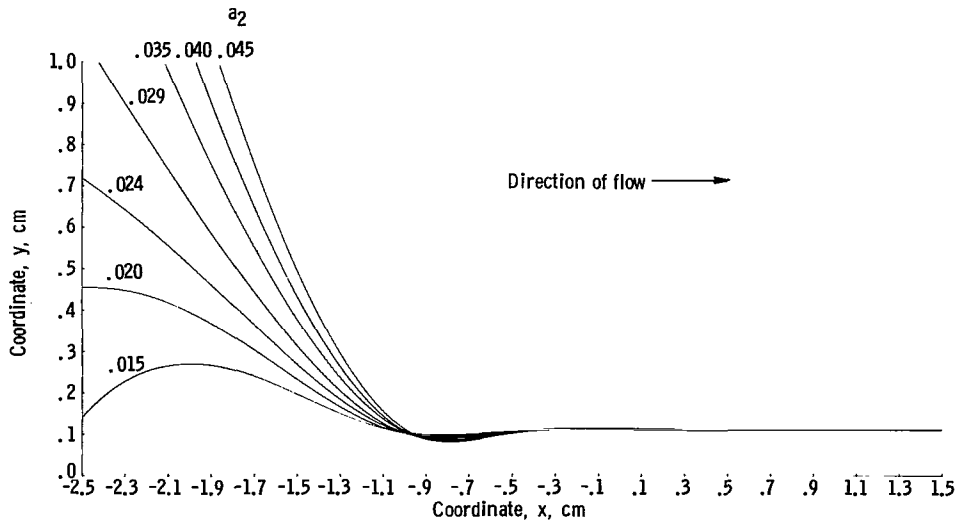


Figure 2. - Family of curves for $A = 0.1569$ produced using Runge-Kutta method.

and (2) since the dynamic contact angle is defined as the angle between the curve and the pipe wall, the curve must asymptotically approach a constant slope for each A , i. e. ,

$$\lim_{q \rightarrow -\infty} \frac{dk}{dq} = -\tan \theta = \text{constant} \quad (18)$$

Of the family of curves generated by equation (16) only one satisfied these boundary conditions. This curve was generated by an a_2 value of 0.029. This was found to be true for all values of A .

It was determined by Friz that the limit in equation (18) varied as a function of A according to the equation

$$\lim_{q \rightarrow -\infty} \frac{dk}{dq} = -2.35 |A|^{1/3}$$

Since the limit is equal to $-\tan \theta$, the contact angle dependence on interface velocity and liquid properties follows directly from this equation. The theoretical relation is

$$\tan \theta = 3.4 \left(\frac{u_o \eta}{\sigma} \right)^{1/3} \quad (19)$$

An independent analysis by Miles (ref. 4) yielded the result that the contact angle depended on interface velocity only up to some critical velocity. Beyond this velocity the contact angle was a constant. This concept is in agreement with the above equation since θ reaches a value that does not change appreciably as the velocity is increased.

EXPERIMENT

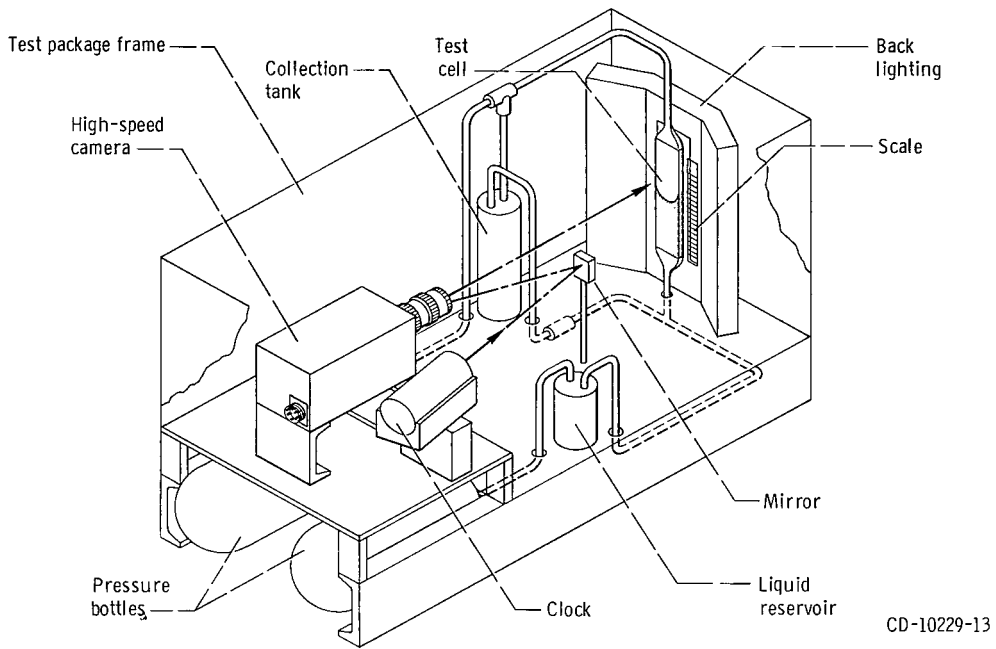
Experiments were conducted under normal gravity conditions to investigate the dynamic contact angle. The intent was to deposit a layer of liquid on the wall of a vertical test cell by withdrawing the liquid from the cell until the interface neared the bottom. The forced return of the liquid over the layer would then produce the desired dynamic contact angle. However, under normal gravity conditions the deposited layer of liquid ran off the walls before the interface could be returned over it. Therefore, in most cases the wall was either dry or covered with an immeasurable thickness. Thus, these experiments were unsatisfactory because the basic assumption of the analysis was not satisfied.

Conducting the experiment in a weightless environment resulted in a nearly stable liquid layer. There, the only force affecting the layer was the surface tension of the liquid. Any run-off or resulting deformity during the available period of weightlessness could not be measured. Lewis Research Center's drop tower was used to produce the weightless environment. A test package containing the experiment was suspended from a wire attached to the top of the tower. Upon release the package fell freely a distance of 24 meters into an arresting box of sand. This corresponded to 2.2 seconds of free fall or weightlessness. During free fall the force due to air drag produced the only acceleration relative to a coordinate system located on the test package. Air drag was reduced to approximately 10^{-5} g's by enclosing the test package inside a drag shield. For the experiment considered here this constituted weightlessness.

Apparatus and Procedure

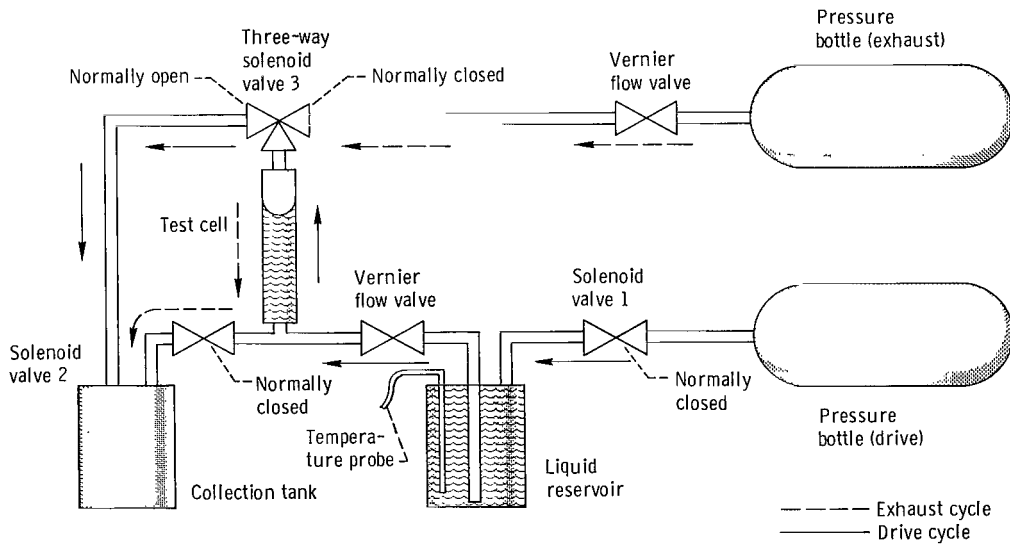
The apparatus used to obtain the experimental data is shown in figure 3. A 20 centimeter length of rectangular glass tubing (1×0.25 cm in cross section) was the test cell in which the dynamic contact angle and interface motion was observed. A high-speed (400 fps), 16-millimeter motion picture camera was used to record the motion of the interface. Included in the camera field of view was a digital clock accurate to ± 0.005 second and a centimeter scale. A thermistor probe located in the liquid reservoir was used to measure liquid temperatures.

A diagram of the flow scheme is shown in figure 4. The pressure bottles were filled



CD-10229-13

Figure 3. - Test package.



CD-10230-13

Figure 4. - Flow diagram.

with nitrogen and were chosen large enough (approximately 5100 cm³) so that the small amount of gas used in the experiment did not affect the pressure. Direction of flow was controlled by the solenoid valves and appropriate time delay relays. The rate of flow was controlled by a combination of vernier flow valve setting and pressure.

Before each test the rectangular glass test cell and all other tubing were thoroughly flushed with the test liquid. The glass test cell was then cleaned ultrasonically. After positioning the liquid vapor interface near the top of the glass tubing, the test package was suspended from the release wire at the top of the drop tower. About 2 seconds before release the camera was turned on. At release the flow cycle was begun. Valves (numbered two and three in fig. 4) were activated allowing the pressure in the "exhaust" bottle to move the liquid down to the bottom of the glass tubing thus depositing the desired liquid layer on the walls. These valves were then deactivated. After a slight delay allowing the interface to stabilize, valve number one was activated and the interface returned at a constant velocity toward its original position. The camera photographed this flow throughout free fall.

The test liquids used in this study are given in table I. Included are the values of the surface tension and viscosity corresponding to the liquid temperature for each test. With the exception of the fluorocarbon solvent, fluid property against temperature data were obtained from standard references. The fluorocarbon properties were obtained from unpublished NASA data. All liquids used had 0° static contact angles on glass. The liquids were either analytic reagent grade or, in the case of the fluorocarbon solvent, precision cleaning grade. A small amount of dye was added to each liquid to improve photographic quality. The dye had no measurable affect on either the viscosity or surface tension.

RESULTS AND DISCUSSION

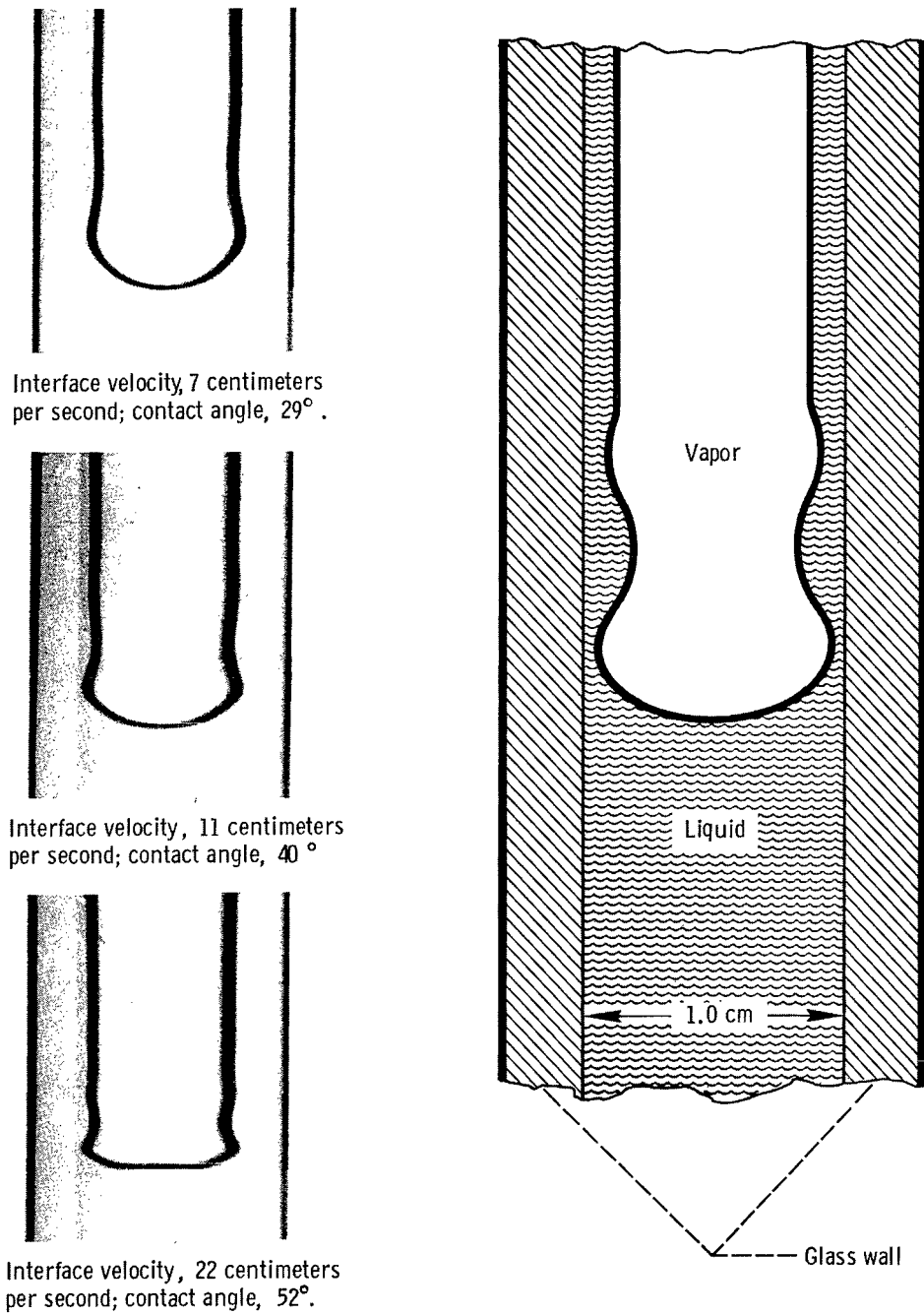
A summary of the experimental data is given in table I. The liquid properties and interface velocities obtained produced dynamic contact angles ranging from 17° to 60°. The contact angles and interface velocities were determined by analyzing four selected frames from each test. Each frame was displayed on a motion analyzer and a graphic plot was made, with the aid of a computer program, reproducing the interface with a magnification of about 100. (Distortion of the interface due to refraction was negligible

TABLE I. - SUMMARY OF LIQUID PROPERTIES AND DATA

Liquid	Temperature, °C	Surface tension, σ , dynes/cm	Viscosity, η , cP	Density, ρ , g/cm ³	Interface velocity, u_0 , cm/sec	$\frac{u_0 \eta}{\sigma}$	Measured tangent, θ	Calculated dynamic contact angle, θ , deg
Ethanol	22.9	22.6	1.14	0.787	2.0	0.0010	0.408	22
	22.8	22.6	1.14	.787	4.4	.0022	.406	22
	22.4	22.6	1.14	.788	5.7	.0029	.516	27
	22.1	22.6	1.15	.788	6.6	.0034	.586	30
	21.2	22.6	1.17	.788	13.5	.0070	.787	38
	22.9	22.6	1.14	.787	17.2	.0087	.821	39
	23.2	22.5	1.13	.787	15.7	.0079	.855	40
	22.0	22.7	1.15	.788	18.3	.0093	.899	42
	22.2	22.6	1.15	.788	18.7	.0095	.914	42
^a FC-43	19.3	16.8	6.71	1.90	1.4	0.0056	0.571	30
	19.3	16.8	6.71	1.90	11.2	.045	1.36	54
	20.5	16.8	6.41	1.90	12.7	.049	1.30	52
	20.8	16.6	6.34	1.90	15.2	.058	1.72	60
Methanol	23.0	22.4	0.56	0.788	5.4	0.0014	0.298	17
	23.0	22.4	.56	.788	10.9	.0027	.468	25
	21.4	22.6	.57	.790	28.3	.0071	1.37	54
1-Butanol	22.9	24.4	2.74	0.807	6.6	0.0074	0.549	29
	22.8	24.4	2.75	.807	11.1	.013	.845	40
	22.1	24.4	2.80	.808	21.6	.025	1.27	52

^aFluorocarbon solvent manufactured by the 3M Co.

because the walls of the test cell were flat and perpendicular to the camera line of sight.) The tangent of the dynamic contact angle was then determined geometrically from these plots (see appendix). The final contact angle datum point was an average value of eight calculated contact angles (i. e., two from each frame). The angles presented are accurate to within a mean deviation of $\pm 4^\circ$. Frames from three typical tests are shown in figure 5. The effect of velocity on the interface shape and waveform is very evident. The interface velocity was determined from a plot of interface position against time. Figure 6 shows a plot of position as a function of time for the three cases presented in figure 5. Velocities were generally constant and accurate to better than 10 percent.



CD-10231-13

Figure 5. - Liquid-vapor interface for butanol showing contact angle for three interface velocities.

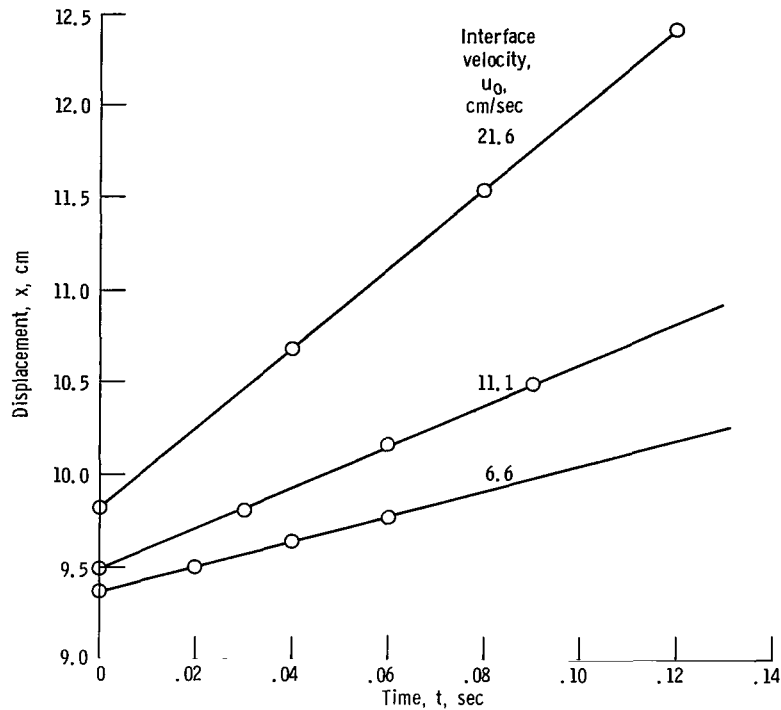


Figure 6. - Interface velocity measurement for three cases shown in figure 5.

A comparison of the data with the theoretical relation (eq. (19))

$$\tan \theta = 3.4 \left(\frac{u_0 \eta}{\sigma} \right)^{1/3}$$

predicted by G. Friz is given in figure 7. This figure is a log-log plot of the $\tan \theta$ against the quantity $u_0 \eta / \sigma$. Thus the above equation is represented by a straight line having a slope of one third. Possible measurement error in $\tan \theta$ is shown for each data point. As can be seen, there is good agreement between theory and experiment. The conclusion, therefore, is that the dynamic contact angle dependence on interface velocity and liquid properties is adequately given by the above equation. The conclusion is also then that layer thickness does not affect the contact angle. Although no specific attempt was made to substantiate this, layer thicknesses were observed to vary from test to test without noticeable effect. The average layer thickness for each test was about 0.1 centimeter.

Further examination of figure 7 indicates, however, a slight trend toward higher contact angles than predicted. A possible explanation may be that there was error in the determination of the interface velocity. Both the method of depositing the liquid layer

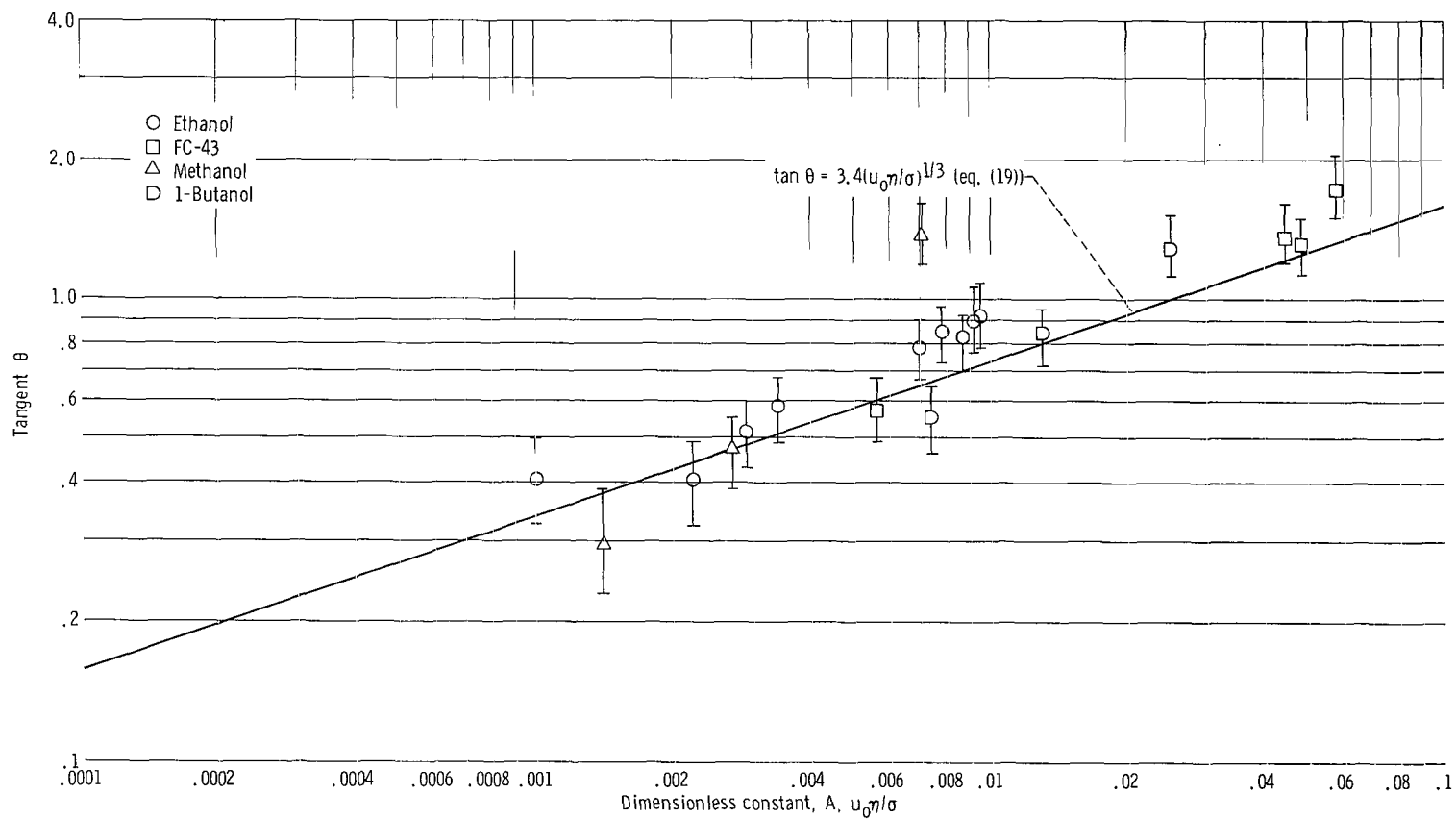


Figure 7. - Dynamic contact angle as function of interface velocity and liquid properties for wetting liquids.

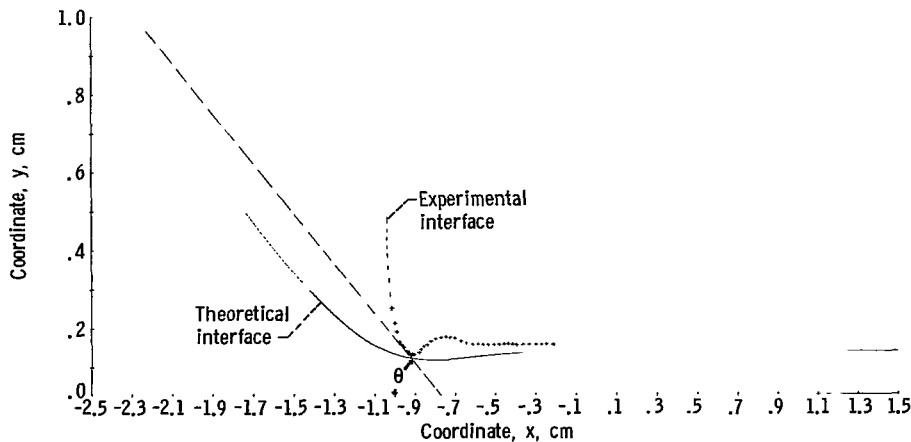


Figure 8. - Theoretical and experimental interface shape for FC-43. Interface velocity, u_0 , 12.7 centimeters per second.

and/or the instability of a layer of constant thickness (the surface tension tends to deform the layer) may have imparted slight downward flow in the wall layer. This would result in a higher relative velocity than actually measured and in most cases would shift the data toward the theoretical curve. Error may also have been introduced by exceeding the condition of creeping motion, that is, Reynolds numbers $\ll 1$. Velocities satisfying this condition could not be used because the accuracy of their measurement was not satisfactory. The Reynolds numbers ranged from about 4 to 400. (The highest Reynolds number corresponds to the datum point falling farthest from the theoretical curve.) The characteristic dimension used in the calculations of the Reynolds number was the average layer thickness of 0.1 centimeter.

Figure 8 is a comparison of the experimental interface shape and that predicted by Friz. Although there is qualitative agreement in the region of interest (both are damped sinusoidal waves), it is obvious that there is considerable discrepancy quantitatively in frequency and amplitude. This was noticed also by Friz upon comparison with his own experimental data on interface shape. He attributed the discrepancy to the fact that acceleration terms were neglected in his analysis. After including those terms he found better agreement with experiment. According to Friz, this revised analysis will be published at a later date.

SUMMARY OF RESULTS

An experiment was conducted to measure the dynamic contact angle θ as a function of interface velocity and liquid properties and to compare the data to the theoretical relation predicted by G. Friz (ref. 2). The dynamic contact angle is defined as the

angle formed at a surface by an advancing liquid-vapor interface as the interface moves relative to that surface. In this case the surface is a wetting layer of the particular liquid being tested. All liquids used exhibited a zero degree static contact angle. Liquid surface tensions σ ranged from 16.6 to 24.4 dynes per centimeter. Viscosities η ranging from 0.56 to 6.7 cP and interface velocities u_0 ranging from 1.4 to 28 centimeters per second resulted in Reynolds numbers between about 4 and 400. The study yielded the following results:

1. The dynamic contact angle change as a function of interface velocity is significant and measurable.

2. The data show that the theoretical relation between contact angle and interface velocity as derived by G. Friz is adequate. The relation is given by the equation

$$\tan \theta = 3.4 \left(\frac{u_0 \eta}{\sigma} \right)^{1/3}$$

The implication that layer thickness has no affect on the contact angle appears to be correct.

3. The predicted waveform preceding the advancing interface agrees qualitatively with the waveform obtained experimentally.

Lewis Research Center,
National Aeronautics and Space Administration,
Cleveland, Ohio, December 10, 1968,
124-09-17-01-22.

APPENDIX - THE DYNAMIC CONTACT ANGLE MEASUREMENT

The dynamic contact angle was measured using a geometric analysis. In a weightless environment, the interface between the wetting layers of liquid was nearly elliptical in shape. The eccentricity of this "ellipse" was unity for the static case and decreased as the interface velocity increased. For the purposes of contact angle definition and measurement only the portions of the interface that could be approximated by sections of circles were considered (see fig. 9).

The contact angle was defined experimentally as the angle between the tangent to each circle at the point of contact with the wall layer and the wall. The point of contact was determined by comparing the curvature of each circle with the curvature of the interface in the wall layer just preceding the first wave. The point at which the curvature changed from one value to the other was taken to be the contact point. Figure 9 shows the interface for butanol plotted from a typical frame of data film. The interface velocity is 21.6 centimeters per second. The center coordinates, (2.33, 11.13) and (2.66, 11.13), of the circles intersecting the interface data points were obtained by averaging the center coordinates of the circles intersecting each consecutive set of three data points. The points considered were for example, A, C, E; B, D, F; C, E, G, etc. The radius of the averaged circle was the average distance from its center to each data point. A tangent

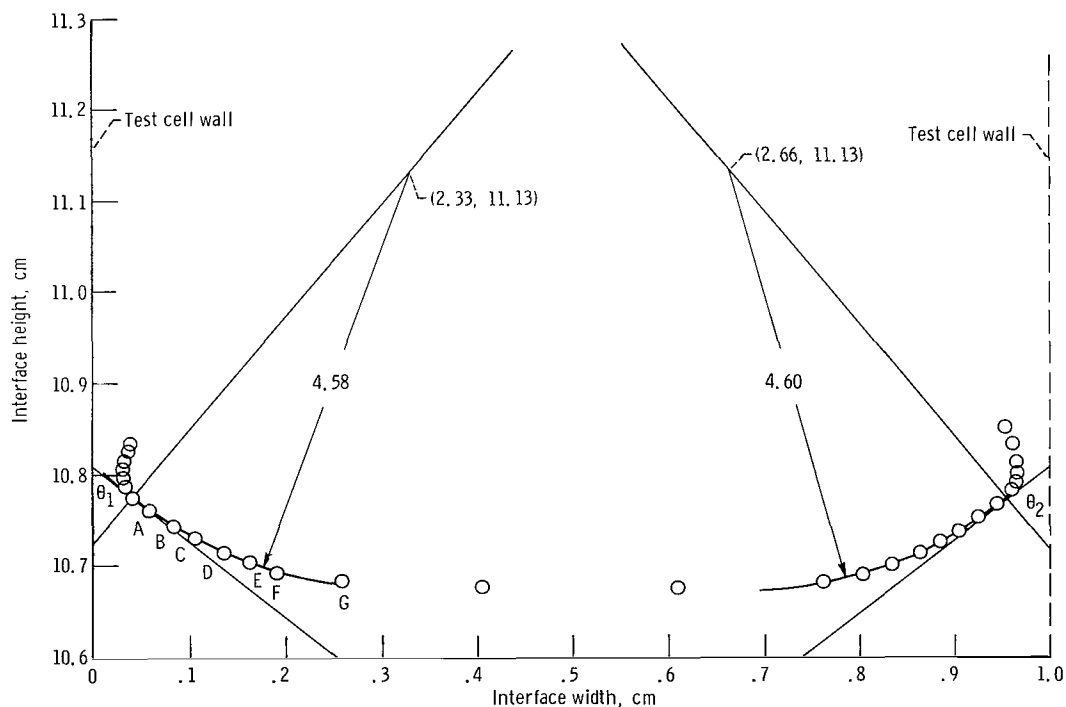


Figure 9. - Contact angle definition and measurement for butanol. Interface velocity, μ_0 , 21.6 centimeters per second. $\tan \theta_1 = 0.252/0.208 = 1.2115$; $\theta_1 = 50.6^\circ$. $\tan \theta_2 = 0.262/0.210 = 1.2470$; $\theta_2 = 51.3^\circ$.

was drawn at the point at which this circle deviated from the data near each wall and the contact angle measured. For the specific case shown, the interface velocity is such that the center of the interface is slightly flattened. It was necessary, therefore, to use a different averaged circle for each side thus neglecting the flat portion of the interface. The two contact angles measured from figure 9 were averaged with six other measurements resulting in an average dynamic contact angle of 52° for an interface velocity of 21.6 centimeters per second. The accuracy of measurement by this method is $\pm 4.0^{\circ}$ (mean deviation).

REFERENCES

1. Rose, W.; and Heins, R. W.: Moving Interfaces and Contact Angle Rate-Dependency. *J. Colloid Sci.*, vol. 17, no. 1, Jan. 1962, pp. 39-48.
2. Friz, Gerhard: Über den dynamischen Randwinkel im Fall der vollständigen Benetzung. *Zeit. für angew. Physik*, vol. 19, no. 4, 1965, pp. 374-378.
3. Abramson, H. Norman, ed.: *The Dynamic Behavior of Liquids in Moving Containers, with Applications to Space Vehicle Technology*. NASA SP-106, 1966.
4. Miles, J. W.: Surface-Wave Damping in Closed Basins. *Proc. Roy. Soc., Ser. A*, vol. 297, no. 1451, Mar. 21, 1967, pp. 459-475.

FIRST CLASS MAIL

NOV 37 41 30S 69058 00903
RESEARCH LABORATORY/AFWL/
KITLAND AIR FORCE BASE, NEW MEXICO 8711

NOV 37 41 30S 69058 00903

POSTMASTER: If Undeliverable (Section 158
Postal Manual) Do Not Return

"The aeronautical and space activities of the United States shall be conducted so as to contribute . . . to the expansion of human knowledge of phenomena in the atmosphere and space. The Administration shall provide for the widest practicable and appropriate dissemination of information concerning its activities and the results thereof."

— NATIONAL AERONAUTICS AND SPACE ACT OF 1958

NASA SCIENTIFIC AND TECHNICAL PUBLICATIONS

TECHNICAL REPORTS: Scientific and technical information considered important, complete, and a lasting contribution to existing knowledge.

TECHNICAL NOTES: Information less broad in scope but nevertheless of importance as a contribution to existing knowledge.

TECHNICAL MEMORANDUMS: Information receiving limited distribution because of preliminary data, security classification, or other reasons.

CONTRACTOR REPORTS: Scientific and technical information generated under a NASA contract or grant and considered an important contribution to existing knowledge.

TECHNICAL TRANSLATIONS: Information published in a foreign language considered to merit NASA distribution in English.

SPECIAL PUBLICATIONS: Information derived from or of value to NASA activities. Publications include conference proceedings, monographs, data compilations, handbooks, sourcebooks, and special bibliographies.

TECHNOLOGY UTILIZATION PUBLICATIONS: Information on technology used by NASA that may be of particular interest in commercial and other non-aerospace applications. Publications include Tech Briefs, Technology Utilization Reports and Notes, and Technology Surveys.

Details on the availability of these publications may be obtained from:

SCIENTIFIC AND TECHNICAL INFORMATION DIVISION
NATIONAL AERONAUTICS AND SPACE ADMINISTRATION
Washington, D.C. 20546